

Carbon doped PDMS: conductance stability over time and implications for additive manufacturing of stretchable electronics

This content has been downloaded from IOPscience. Please scroll down to see the full text.

2017 J. Micromech. Microeng. 27 035010

(<http://iopscience.iop.org/0960-1317/27/3/035010>)

View [the table of contents for this issue](#), or go to the [journal homepage](#) for more

Download details:

This content was downloaded by: cmajidi

IP Address: 128.237.205.5

This content was downloaded on 16/05/2017 at 15:14

Please note that [terms and conditions apply](#).

You may also be interested in:

[Fabrication methods and applications of microstructured gallium based liquid metal alloys](#)

M A H Khondoker and D Sameoto

[Printable stretchable interconnects](#)

Wenting Dang, Vincenzo Vinciguerra, Leandro Lorenzelli et al.

[Smart fabric sensors and e-textile technologies: a review](#)

Lina M Castano and Alison B Flatau

[Dielectric elastomer actuators fabricated using a micro-molding process](#)

Aaron P Gerratt, Bavani Balakrisnan, Ivan Penskiy et al.

[Thermal cure effects on electromechanical properties of conductive wires by direct ink write for 4D printing and soft machines](#)

Quanyi Mu, Conner K Dunn, Lei Wang et al.

[Stretchable gold conductors](#)

T Adrega and S P Lacour

[Elastomeric composites based on carbon nanomaterials](#)

Sherif Araby, Qingshi Meng, Liqun Zhang et al.

[Highly elastic conductive polymeric MEMS](#)

J Ruhhammer, M Zens, F Goldschmidtboeing et al.

[A review of the hybrid techniques for the fabrication of hard magnetic microactuators based on bonded magnetic powders](#)

M Pallapa and J T W Yeow

Carbon doped PDMS: conductance stability over time and implications for additive manufacturing of stretchable electronics

Mahmoud Tavakoli¹, Rui Rocha¹, Luis Osorio¹, Miguel Almeida¹, Anibal de Almeida¹, Vivek Ramachandran², Arya Tabatabai², Tong Lu² and Carmel Majidi²

¹ Institute of Systems and Robotics, University of Coimbra, Portugal

² Soft Machines Lab, Carnegie Mellon University, PA, United States of America

E-mail: mahmoud@isr.uc.pt and cmajidi@andrew.cmu.edu

Received 21 October 2016, revised 12 December 2016

Accepted for publication 19 January 2017

Published 8 February 2017



CrossMark

Abstract

Carbon doped PDMS (cPDMS), has been used as a conductive polymer for stretchable electronics. Compared to liquid metals, cPDMS is low cost and is easier to process or to print with an additive manufacturing process. However, changes on the conductance of the carbon based conductive PDMS (cPDMS) were observed over time, in particular after integration of cPDMS and the insulating polymer. In this article we investigate the process parameters that lead to improved stability over conductance of the cPDMS over time. Slight modifications to the fabrication process parameters were conducted and changes on the conductance of the samples for each method were monitored. Results suggested that change of the conductance happens mostly after integration of a pre-polymer over a cured cPDMS, and not after integration of the cPDMS over a cured insulating polymer. We show that such changes can be eliminated by adjusting the integration priority between the conductive and insulating polymers, by selecting the right curing temperature, changing the concentration of the carbon particles and the thickness of the conductive traces, and when possible by changing the insulating polymer material. In this way, we obtained important conclusions regarding the effect of these parameters on the change of the conductance over time, that should be considered for additive manufacturing of soft electronics. Also, we show that these changes can be possibly due to the diffusion from PDMS into cPDMS.

Keywords: stretchable electronics, conductive PDMS, 3D printed electronics, carbon black

 Supplementary material for this article is available [online](#)

(Some figures may appear in colour only in the online journal)

1. Introduction

Electronics that are intrinsically soft and stretchable have the potential to revolutionize the way in which humans physically interact with machines. By matching the compliance, elasticity, and density of human tissue, soft electronics could adhere to the skin or be incorporated into clothing without causing discomfort or constraining natural motion. In recent

years, a broad range of materials, composites, and so-called ‘deterministic’ micro-patterned architectures have been introduced to support soft and stretchable electronic functionality [1]. These include conductive textiles composed of Ag-coated elastane fabrics (e.g. MedTex P-130; Statex), spray-deposited films of SWCNT on an elastomer substrate [2], microfluidic channels of liquid-phase metal embedded in polydimethylsiloxane (PDMS) [3], and wavy circuits

composed of pre-buckled or serpentine Au and Cu wiring [4]. Also Graphene-Metal hybrid structures were introduced for transparent and stretchable electrodes [5, 6]. Another common approach is to use conductive rubber composites composed of elastomers filled with percolating networks of conductive microparticles, ranging from Ag microflakes in a fluoropolymer [7] to acetylene carbon black (CB) in polydimethylsiloxane (PDMS) [8, 9].

Among these existing soft electronic materials, CB-filled conductive PDMS (cPDMS) elastomers are particularly attractive for their intrinsic mechanical properties—soft (elastic modulus ~ 1 MPa), highly stretchability (above 100% strain), and low density (~ 1 g cm⁻³)—low cost, and ease of manufacturability through laser patterning [10], screen printing, and additive manufacturing (e.g. syringe-based 3D printing). Although polymers are usually electrically insulating, by adding conductive particles—such as CB—into the polymer matrix it is possible to create some conductive paths and undergo a insulator–conductor transition [11]. These conductive paths can be achieved from two different mechanisms: mechanical contact between conductive particles; and the electron tunneling effect—when the particles are not in touch but close enough to enable the flowing of electrons through the polymer matrix [12]. However, in spite of their promise as an inexpensive and versatile material for wearable electronics, cPDMS requires a high concentration of CB and, even so, the conductivity is relatively poor. Despite this fact, it is still possible to produce flexible applications based on these composites [13]. On the other hand, to reduce the amount of CB particles needed to make the polymer conductive, it is possible to use multiphase polymers blends. Due to the multiple phase of the polymer it is possible have a selective distribution of CB making it conductive at a lower filler content [14].

Furthermore, beyond the electrical characteristics of CB, it can also be used as reinforcing agents for elastomers and rubbers, increasing the tensile strength at breaks, the abrasion resistance and fatigue properties [15]. Figure 1 shows one of the applications of the all-elastomer stretchable sensors which are embedded in the fingers of the new versions of ISR-Softband [16] and the UC-Softband [17, 18]. Patterned geometries of cPDMS are embedded inside an elastomeric skin in order to measure the pressure on the finger tip and bending of the joints. Soft pressure sensors might be used in different applications such as soft robots for minimally invasive surgery [19] and in general for Soft Robotics Microsensing [20]. During our experiments to integrate cPDMS composites for pressure sensing, we found that cPDMS can suffer from significant loss of conductance over time. In particular, using screen printing, stencil lithography, or 3D printing to combine uncured cPDMS and insulating PDMS, we observed loss of conductance in the embedded cPDMS traces over time. This particularly happens after integration of insulating polymers into the cPDMS. The loss of conductance can occur for a period of several days to several months and in some cases, the reduction in the conductance of the composite continues until it drops below the percolation threshold and loses conductance. In this manuscript, we examine the change in

conductance of cPDMS traces embedded in insulating PDMS. We produce samples with stencil lithography and casting as these are among the most popular, rapid, and inexpensive ways of producing cPDMS-based electronics. Specifically, we created custom masks and molds to produce several sensing elements with different combinations of insulating polymers, curing methods, CB concentration, and geometry. We show that by appropriate selection of these parameters, it is possible to produce reliable and long lasting cPDMS that would keep their conductance constant for long periods. These findings are useful for different fabrication methods including soft lithography, screen printing, 3D printing, and other methods in which conductive and insulating elastomer are deposited while still in their uncured state.

2. Experimental method

The purpose of this study is to understand the reason behind the changes on the conductance of the cPDMS and, based on that, suggest methods to minimize the conductance loss. We observed that the changes on conductance happen after curing the cPDMS and after integrating the cPDMS on the PDMS. In some cases, the resistance of a pattern became stable after a couple of hours. However, in some other cases, the resistance increased over the course of several days, up to the point of sometimes the conductive traces/electrodes becoming non-conductive. The goal of this study is to understand the effect of materials and fabrication process parameters on the conductance of the cPDMS over time and to suggest a fabrication process that results in stable conductivity over time.

2.1. Materials

The cPDMS was produced by mixing PDMS (Sylgard 184; 10:1 base-to-catalyst ratio; Dow Corning) with acetylene CB powder (Alfa Aesar). The minimum weight percentage of CB necessary for conductivity was found to be around %12wt. In the experiments, we tried two compositions based on 16% and 25% weight of carbon black. EcoFlex 00-30 and PMC Urethane (smooth on) were both produced by mixing part A and part B in equal amounts by volume or weight.

For concentrations larger than 25%wt, the material becomes too viscous for processing and filling the molds. Thus, 25%wt was the highest concentration considered in this study. To decrease the viscosity, we used either acetone or Hexane (Chem-Lab) to the silicone and the CB mixture to make it less viscous. The composition was mixed for 1 h in a magnetic stirrer. We performed a test in order to verify the consistency of the mixtures. After preparation of the mixture, we prepared a thin film with a thin film applicator (ZUA 2000 Universal Applicator; Zehntner). The film was then cured in an oven for 10 min at 120 °C. 10 equal traces (30 × 3 × 1) mm were cut, with a 30W carbon dioxide laser cutter (VLS 3.50; Universal Laser Systems, Inc.). We then measured the resistance of the traces using a multimeter. Table 1 shows the values measured which demonstrates a good dispersion

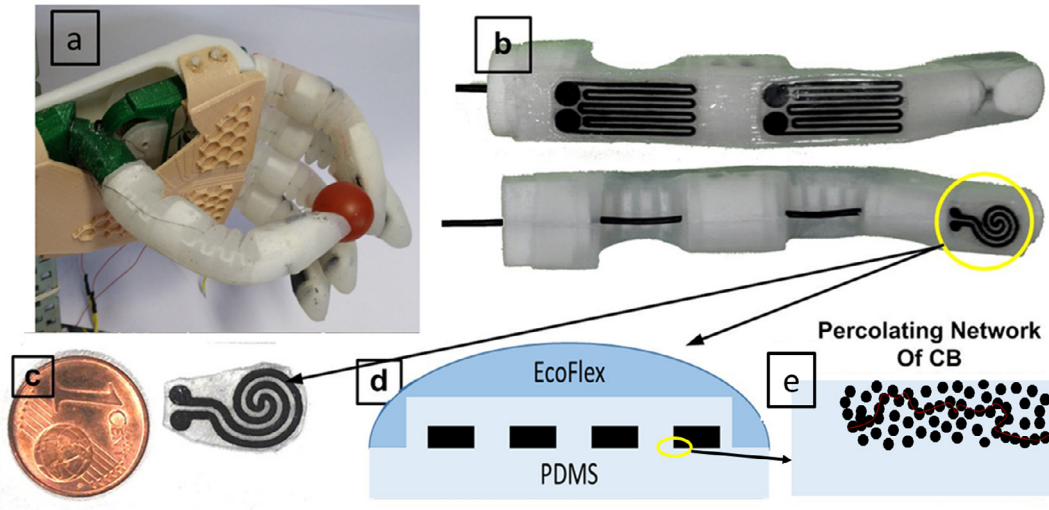


Figure 1. (a) The new version of the ISR-SoftHand with embedded pressure sensors. (b) Soft elastomeric fingers with all elastomer pressure and bending sensors. (c) An example of a pressure sensor before integration into the hand. (d) The sensor is composed on patterned cPDMS sandwiched between layers of PDMS and is then embedded in an EcoFlex substrate. (e) Percolating networks of CB inside the PDMS assures conductivity of the cPDMS traces.

Table 1. Consistency of mixture.

Sample	$R_{\text{acetone}}(\text{K}\Omega)$	$R_{\text{hexane}}(\text{K}\Omega)$
1	2.29	2.16
2	2.28	2.23
3	2.27	2.11
4	2.31	2.16
5	2.32	2.19
6	2.19	2.21
7	2.30	2.18
8	2.26	2.13
9	2.30	2.19
10	2.28	2.14

for both mixtures. Samples that contain acetone showed an average resistance of 2.28 k Ω and a standard deviation of 0.03 k Ω . These values were 2.17 k Ω and 0.04 k Ω for samples containing hexane. We also noticed that compared to acetone, higher amount of hexane can be absorbed by the mixture.

2.2. Fabrication

The general fabrication method for every conductive trace is based on integration of patterned cPDMS with an insulating polymer (PDMS, EcoFlex, Urethane). This was done either by surface printing through a stencil, or by lifting from a laser patterned mold. For the lifting process molds were produced by engraving an acrylic sheet (figures 2(a) and (c), molds A and B, respectively). For the surface printing (figure 2(e)), a stainless steel stencil was produced by a laser cutter(mold C).

We fabricated conductive traces with different dimensions, insulating materials and process. All electrodes are fabricated either by first creating a layer of an insulating polymer and then depositing the cPDMS using the patterned molds,

or by first filling the molds with cPDMS and then pouring the insulating pre-polymer over it. In summary, conductive traces were produced using three different techniques in order to reflect the differences in the curing order, i.e. PDMS first, cPDMS first, or both cured together:

- Stencil lithography in which PDMS is cured first (130 °C for 25 min) and then uncured cPDMS is deposited using a stainless steel stencil. The excess cPDMS is cleaned in such a way that when the stencil is removed, only the desired pattern remains over the PDMS layer. Both layers are then cured at 130 °C for 25 min or at room temperature for 48 h. (figure 3(a)).
- Referring to figure 3(b), acrylic mold is first filled with cPDMS. After the excess is removed, the cPDMS is cured at 130 °C for 25 min. Lastly, a PDMS layer with a thickness of 0.5 mm is added on top of the cPDMS and is cured at room temperature for 48 h or again in the oven under the same conditions.
- Referring to figure 3(c), the mold is first filled with cPDMS and the excess is carefully removed. In this method, it is impossible to clean the mold afterwards, meaning that it is imperative to clear all the material that may create shortcuts between the paths before pouring the final layer of PDMS. The sample is then either cured in the oven at 130 °C for 25 min or placed at room temperature to cure for 48 h.

The width \times thickness dimensions (in mm) of the cPDMS channels for each developed sample are: (0.6, 1.5, 3) \times (0.25, 0.3, 0.4) and (1.5, 3) \times (0.35, 0.4, 0.6, 0.9)

2.3. cPDMS and PDMS integration

Figure 4(a) shows a close-up picture of some of the samples. Using the molds from figure 2, 148 different conductive traces were built and extensive tests concerning their resistance were

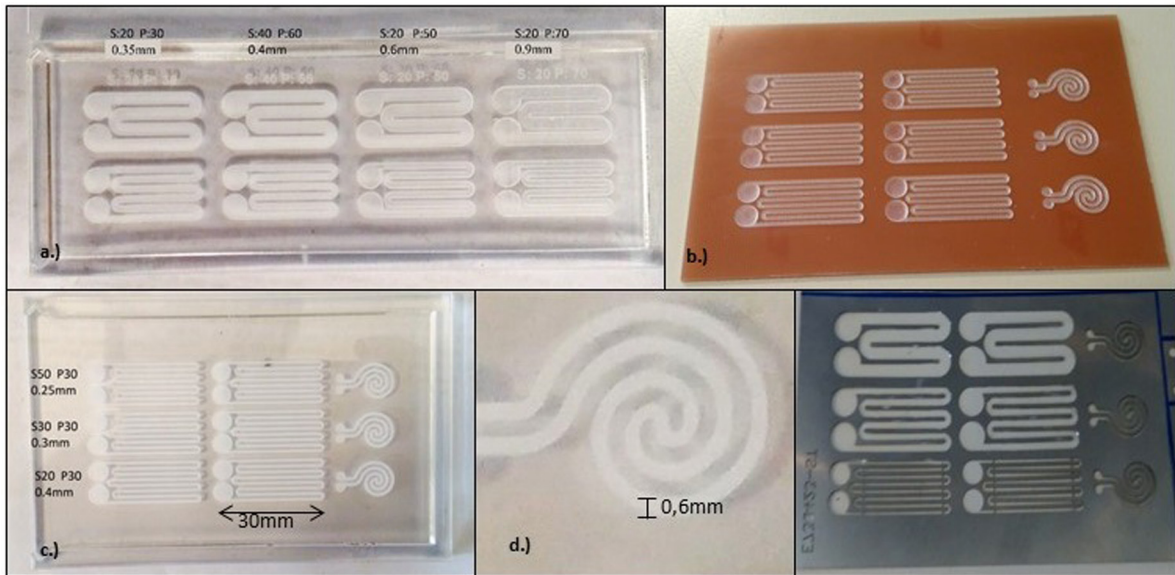


Figure 2. Molds used to make the cPDMS patterns. (a) Acrylic mold made using a laser-cutting machine (‘S’ refers to the laser speed and ‘P’ to its power) to engrave patterns with dimensions (1.5, 3) × (0.35, 0.4, 0.6, 0.9) mm. (b) Mold made in the back of a PCB using a CNC to engrave the patterns. (c) Acrylic mold made using a laser-cutting machine to engrave patterns with dimensions (0.6) × (0.25, 0.3, 0.4) mm. (d) Close-up of a spiral pattern. (e) Mold made from a 0.1 mm stainless steel sheet (stencil).

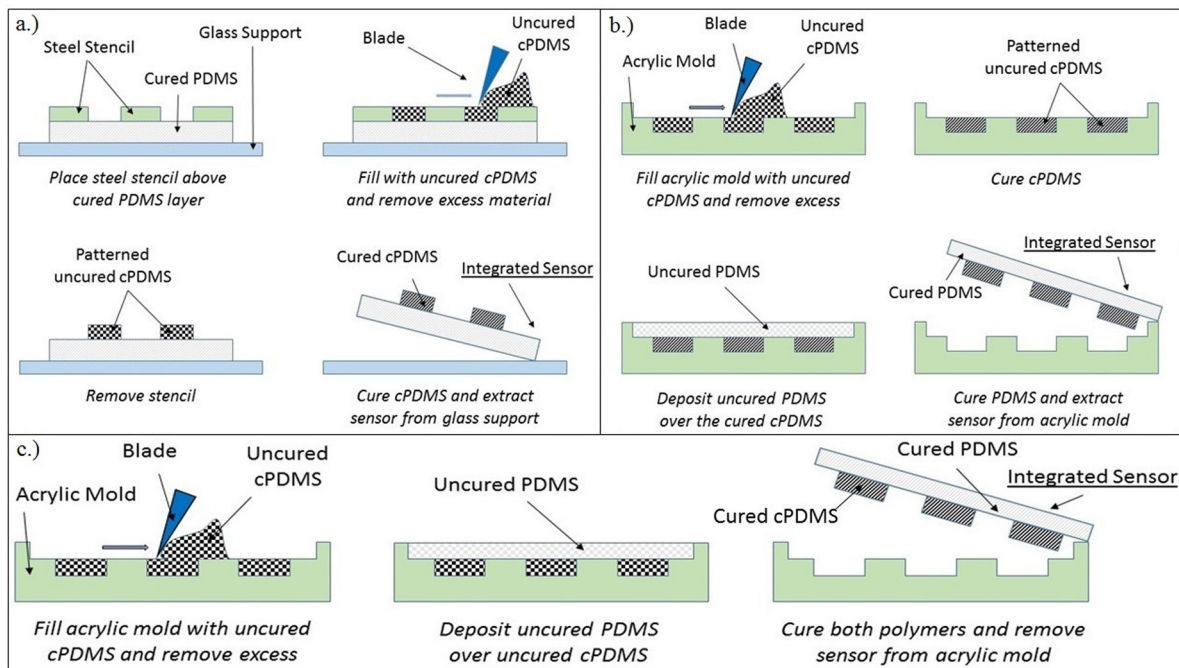


Figure 3. Schematics depicting each of the fabrication methods. (a) Curing PDMS first. (b) Curing cPDMS first. (c) Curing PDMS and cPDMS at the same time.

performed. The resistance of the samples was measured at specific instances (fresh, cured and integrated) and over time, at 24h intervals over a six days period, and then the test was repeated after three months.

- Fresh—right after mixing the composition and casting it into the mold;
- Cured—right after curing the cPDMS (not applicable if PDMS and cPDMS are cured together);

- Integrated—right after integration and curing of the PDMS layer (if cured in the oven, a waiting period of 30 min is given for the sample to cool down);
- Over time—every 24h after integration.

Measurements of the conductive traces are presented in figures 5 and 6 and demonstrate the influence of CB concentration, sample thickness, and curing method. The curing methods are defined as the following:

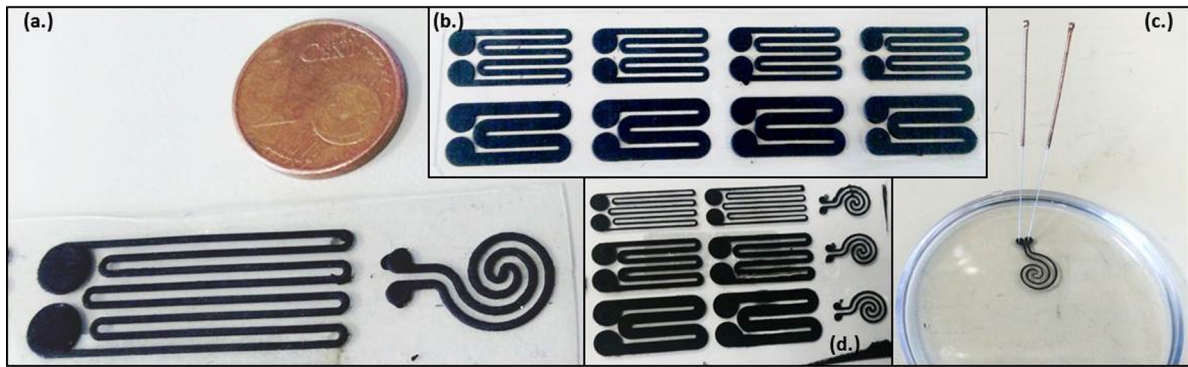


Figure 4. Examples of the produced samples. (a) Close-up of the two types of samples tested. (b) Conductive traces developed in acrylic molds. (c) Measuring the resistance of a spiral sample using a pair of acupuncture needles. (d) Electrodes made using the CNC-milled PCB (notice the irregularities on the cPDMS tracks).

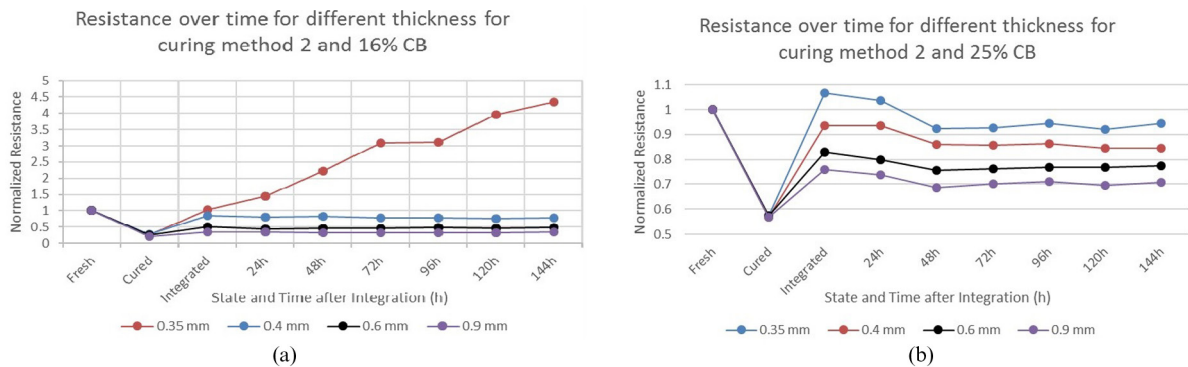


Figure 5. (a) Dependence of the normalized resistance (to the fresh value) on the thickness of the conductive trace (linear with 1.5 mm Width) for the curing method 2 and 16% carbon case. (b) Dependence of the normalized resistance (to the fresh value) on the thickness of the conductive trace (linear with 1.5 mm width) for the curing method 2 and 25% carbon case. The resistance drop from the fresh to cured value is due to the evaporation of the solvents. After cPDMS is cured in all cases the resistance increases compared to the cured value. It can be seen in both plots that when the sample is thinner the change of the resistance is higher. Also by comparing the two plots, one can see that the resistance of the cPDMS with lower carbon concentration is increasing more than the one with more carbon concentration on PDMS.

- (1) Method 1—first cure a layer of cPDMS alone in the oven for 25 min at 130 °C and then add on top of it a layer of uncured PDMS. Cure the two layers in the oven for 25 min at 130 °C;
- (2) Method 2—first cure a layer of cPDMS alone in the oven for 25 min at 130 °C and then add on top of it a layer of uncured PDMS. Cure the two layers at room temperature for 48 h;
- (3) Method 3—cure cPDMS and PDMS at the same time in the oven for 25 min at 130 °C;
- (4) Method 4—cure cPDMS and PDMS at the same time at room temperature for 48 h;
- (5) Method 5—first cure a sheet of PDMS and then use the steel stencil molds to print the cPDMS on top of it. Take everything to cure in the oven for 25 min at 130 °C;
- (6) Method 6—first cure a sheet of PDMS and then use the steel stencil molds to print the cPDMS on top of it. Take it to cure at room temperature for 48 h.

To be able to compare the changes on the resistance, all the lines in the plots were normalized by their corresponding fresh value. Due to the nature of methods 3, 4, 5 and 6, where the curing and integration develop at the same time, it was impossible to measure the cured resistance values of the cPDMS, and thus these values were omitted in the respective plots.

3. Results and discussion

In this section we discuss the obtained results in details.

3.1. Conductive traces resistance

The resistance of the conductive traces was measured by a digital multi-meters through needles inserted into the cPDMS (figure 4). Needles were not removed and re-inserted during the readings of the resistance. On the presented values in this paper, the contact resistance is not excluded. Nevertheless, the goal is to monitor the changes of the resistance over time, and therefore the contact resistance does not affect conclusions of this study. In case of figure 8, the resistance value was transmitted continuously through a Bluetooth module. Whenever it was possible to obtain the cured value, it became apparent that the resistance of the cPDMS pattern always decreased after curing in relation to the freshly made uncured cPDMS, as is exemplified in figure 5. This is due to the evaporation of some of the chemicals in the composition during the curing process which causes an increase in concentration of carbon microparticles. To track the changes on the resistance of the traces, the actual comparison should be between the resistance value of the traces right after curing and then over time.

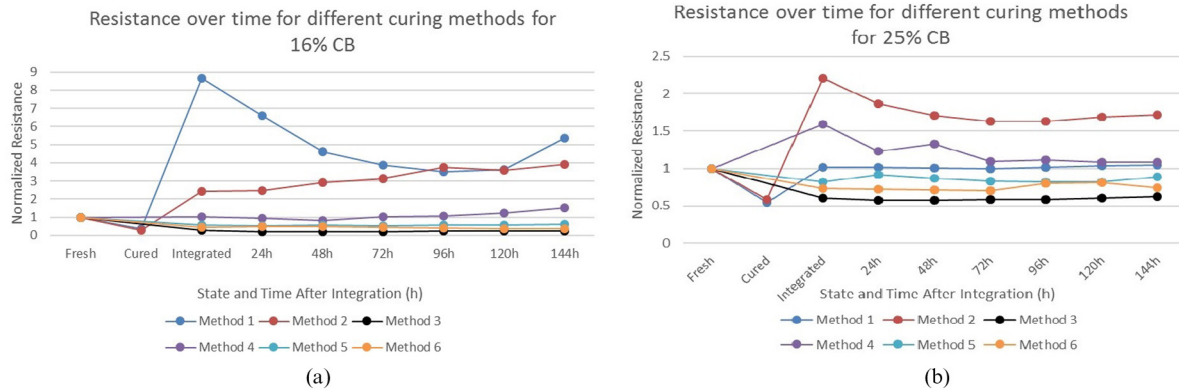


Figure 6. Left plot: dependence of the normalized resistance (to the fresh value) on curing method for a 16% carbon 0.6×0.25 mm linear sample. Right plot: dependence of the normalized resistance (to the fresh value) on curing method for a 25% carbon 0.6×0.25 mm linear sample.

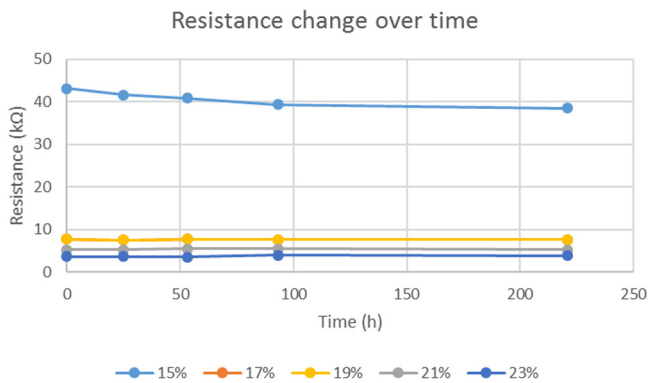


Figure 7. Plot of the variation of the resistance over 220 h.

As can be seen in figure 5, it is actually the integration stage that causes an increase in the resistance from the cured value. (This is when cPDMS and PDMS are put in contact.) This is probably because the cPDMS becomes less concentrated in carbon particles, when it get in touch with PDMS.

3.1.1. Influence of thickness. Figure 5 shows the effect of the thickness of the traces on the change of the conductivity over time. The thinner the cPDMS track is, the higher is the rate of the increase of the resistance, after integration with the PDMS. This is probably because the material exchange between PDMS and cPDMS happens mostly at the boundary between both polymers and the neighboring regions. As the distance grows from the contacting surfaces, the carbon concentration of the corresponding layers is less affected. If the region not affected by the diffusion is much larger than the one that is, the influence of the diffusion is lessened. Therefore, thinner traces are more prone to loss of the conductivity than the thicker ones. This can be further observed across both tables S1 and S2 (stacks.iop.org/JMM/27/035010/mmedia). Furthermore, small thicknesses, at times, may introduce some instability in the traces conductance as can be seen in the left plot of figure 5 where the 0.35 mm thickness does not exhibit a well-defined plateau.

3.1.2. Influence of concentration gradient. By comparing the same lines between the left and right plots in figures 5 and

Table 2. Parameters.

Parameter	Variation
cPDMS layer (Width \times thickness) (mm)	$0.6 \times (0.25, 0.30, 0.40)$ $1.5 \times (0.25, 0.35, 0.40, 0.60, 0.90)$ $3 \times (0.25, 0.35, 0.40, 0.60, 0.90)$
Carbon percentage	16%wt 25%wt
Curing order	cPDMS first PDMS first Both together
Temperature	At 130 °C for 25 min At room temperature for 48 h

6, and specially by looking at the thinnest sample (0.35 mm), it can be seen that the loss of conductivity is more visible in the sample with lower carbon concentration. On the lower concentration of CB in cPDMS, and when the percolation threshold is passed only slightly, a small material migration between cPDMS and PDMS, can immediately drop the CB percentage below the percolation threshold. However for higher concentration of CB, the molecules migration has a smaller impact on conductivity. But increasing the percentage of the CB is not always desired, since it changes the mechanical properties of the cPDMS. It is normally desired to reach the percolation threshold with the lowest amount of added particles.

3.1.3. Influence of curing temperature, order, and time. These three factors also have a significant effect on the overall conductance of the traces (see figure 6). For instance, it can be seen that adding uncured PDMS on top of cured cPDMS (methods 1 and 2) has a worse effect when compared to the situation in which uncured cPDMS is deposited over cured PDMS (methods 5 and 6). This situation is not limited to the particular conditions of figure 6 since careful examination of tables S1 and S2 reveals the trend repeats itself for different electrodes parameters. The fact that adding the uncured PDMS over cPDMS has a worse effect than the converse method, suggests that either the uncured PDMS is able to creep into the CB aggregation of cPDMS, or the

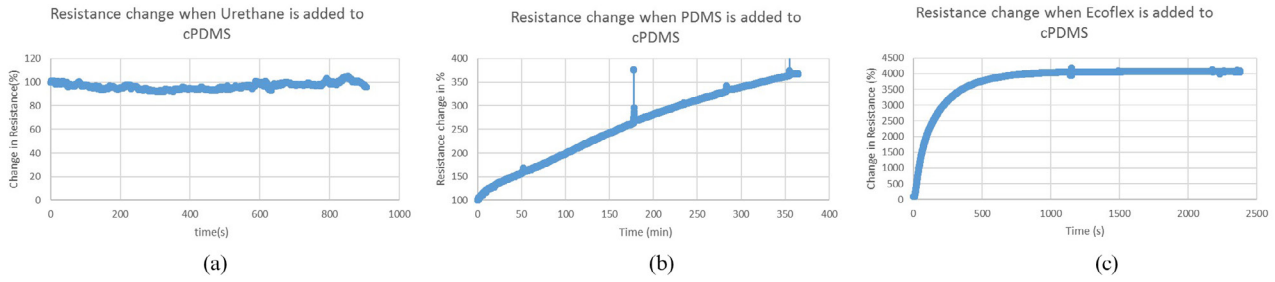


Figure 8. Changes in electrical resistance when the uncured (a) Urethane, (b) PDMS and (c) EcoFlex are added to previously cured cPDMS.

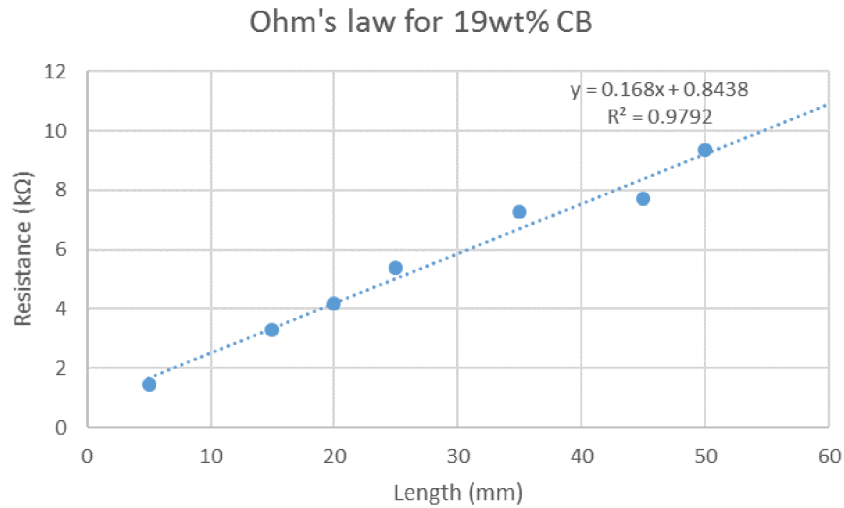


Figure 9. Validation of second Ohm's law for cPDMS.

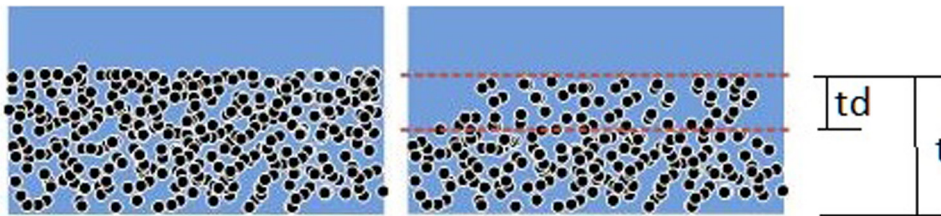


Figure 10. t shows the overall thickness of the patterned cPDMS and t_d shows the diffusion depth after integration of the PDMS, thus impairing the percolation of CB in the border layers.

CB aggregations of cPDMS can move into the lower viscosity PDMS. The effect of the curing order can be studied by comparing only the methods in figure 6 that share the same curing temperature and time, that is, methods 1, 3 and 5 (in which the samples are cured in an oven), and methods 2, 4 and 6 (in which the samples are cured at room temperature). In the first set, samples built by curing the PDMS and the cPDMS (method 3) together always performed the best. In the second set, where all materials are cured at room temperature, method 6 (cure first PDMS and then pour cPDMS over it), was the one that exhibited the best results. In its uncured form, cPDMS is essentially carbon particles in suspension within uncured PDMS. When uncured PDMS and uncured cPDMS are integrated together, they are still in liquid phase and the diffusion that occurs is mostly of PDMS going back and forth between the uncured polymers. The carbon particles, which are much larger than the pre-polymers PDMS

molecules, remain relatively unmoved, causing the net effect of the diffusion to be reduced and thus limiting it. For short curing periods, this is the main reason why method 3 is also the best method among all six methods. However, if the duration increases, the net effect starts to become more noticeable and the resistance of the conductive traces begins increasing relatively to the corresponding fresh value. That is why method 6 actually becomes the best approach in the second set of methods.

In order to correctly analyze the effect of curing temperature and time on the samples, we should only compare method pairs that share the same curing order: methods 1 and 2 (first cure cPDMS and then cure PDMS), methods 3 and 4 (cure PDMS and cPDMS at the same time), and methods 5 and 6 (first cure PDMS and then cure cPDMS). As seen in the right plot from figure 6, methods 1, 3 and 6 were always better than methods 2, 4 and 5, respectively. By increasing the

Table 3. Depth of diffusion, t_d , for method 1.

t_0 (mm)	R_{cured}	$R_{72\text{ h}}$	t_f (mm)	t_d (mm)
0.25	2.97	3.12	0.02	0.23
0.30	0.93	3.76	0.07	0.23
0.40	0.57	1.44	0.16	0.24

temperature and reducing the curing time, we are actually limiting the diffusion time. This is the main reason why methods 1 and 3 are better than methods 2 and 4. Methods 5 and 6, are not different, and in both cases the change of the resistance is minimum. This shows that curing PDMS before integration of the cPDMS, is a good practice.

4. Analysis of the results and discussion

In this section we further analyze the results. We first discuss a bit further the diffusion hypothesis as a possible reason for the change of the resistance of the cPDMS electrodes and how these results can be used in order to improve the fabrication process of the cPDMS based traces, for reliable and long lasting conductive traces whose resistance stays constant during a long time.

The variations observed in the electrical conductivity of cPDMS samples suggest that a material migration or diffusion is the most convincing hypothesis as the reason for loss of the conductivity. Such diffusion at the boundary between the PDMS and cPDMS is responsible for increasing resistance of the cPDMS over time. In order to investigate other factors, such as the effect of environmental factors such as oxidization, solvent effects, etc, we performed another test. We fabricated one trace of cPDMS (0.5 mm \times 2 mm \times 45 mm) for different CB concentrations without combining them with any insulator polymer and measured the resistance for 220 h. As can be seen in figure 7 results show that the resistance did not change over 220h, except for the 15% sample, in which the resistance slightly decreased. This shows that other environmental factors do not change the resistance of the samples, and such changes happens only when the cPDMS gets in touch with PDMS.

The variations overtime observed in the resistance values are indicative of changes in carbon concentration within the cPDMS which, in turn, may be a product of the way diffusion develops. A drop in conductivity implies that either PDMS is creeping into the cPDMS or that conductive material (CB aggregations) is leaving the cPDMS. The former theory is more probable, because if no external work is applied (e.g. mixing), the solid and relatively large CB particles cannot break their bond with adjacent particles and leave the aggregated network. Also, CB particles cannot easily travel inside the high viscosity polymer. Also, it should be mentioned that most of the parameters in table 2 have an effect in the way diffusion interacts with the conductance of the samples: a large thickness provides more robustness against the carbon loss/PDMS gain; when we change the curing order, we are actually changing the diffusion couple which means the curing order gives rise to

Table 4. Depth of diffusion, t_d , for method 2.

t_0	R_{cured}	$R_{72\text{ h}}$	t_f (mm)	t_d (mm)
0.35	0.11	1.16	0.03	0.32
0.40	0.09	0.27	0.13	0.27
0.60	0.04	0.09	0.30	0.30

different D coefficients. Curing temperature and time have a direct impact in the D parameter and Fick's second law, respectively.

We then tested the addition of two different insulating stretchable polymers to evaluate the results. In addition to PDMS, we opted for PMC Urethane and EcoFlex 30 (both for smooth-on). cPDMS was cured first and uncured PDMS, Urethane, and EcoFlex were added to it. We let the samples cure at the room temperature. As can be seen in figure 8, and as we expected, when combined by Urethane, the conductivity of the cPDMS remains constant. The reason behind this is that the bonding between PDMS and Urethane is generally poor. But EcoFlex presents the poorest results and conductivity of the cPDMS in contact with EcoFlex decreases substantially. EcoFlex bonds well with PDMS, but in addition, the curing process of EcoFlex is affected by CB. That is, when EcoFlex is mixed with CB, it does not cure. For this reason, when adding EcoFlex to cPDMS, the EcoFlex in touch with cPDMS stays liquid and can diffuse for a longer time, compared to PDMS. Once more this shows that the bonding stage between the polymers is the reason behind the loss of the conductivity.

Independent from the reason behind the loss of conductivity over time, it is shown that it is possible to minimize this effect in order to fabricate conductive traces that are reliable over a long period.

5. Effect of other factors

As mentioned, it seems that the change of the conductance on the samples is due to some kind of material exchange between the conductive and insulating polymers.

5.1. The diffusion depth

We first evaluate if the second Ohm's law is valid for the cPDMS tracks. To do so it was patterned ten traces of cPDMS (19 wt%) with lengths from 5 to 50 mm and with constant width and thickness, 2 mm and 0.5 mm respectively. As expected, the increase of length led to a linear increase of resistance, figure 9.

Figure 10 shows how diffusion impairs the percolation in the cPDMS layers that are joined to PDMS. Since cPDMS and PDMS bond together strongly, it will be difficult to unbound them and examine the cross section with microscopy. However, we try to estimate the diffusion depth by a comparative study.

If we consider samples with 16% of CB, we can assume that small amounts of the diffusion on layers of cPDMS drops the CB percentage below the conductivity threshold and become non conductive. Here we define t_d as the effective depth of the diffusion. That is, if we are able to calculate

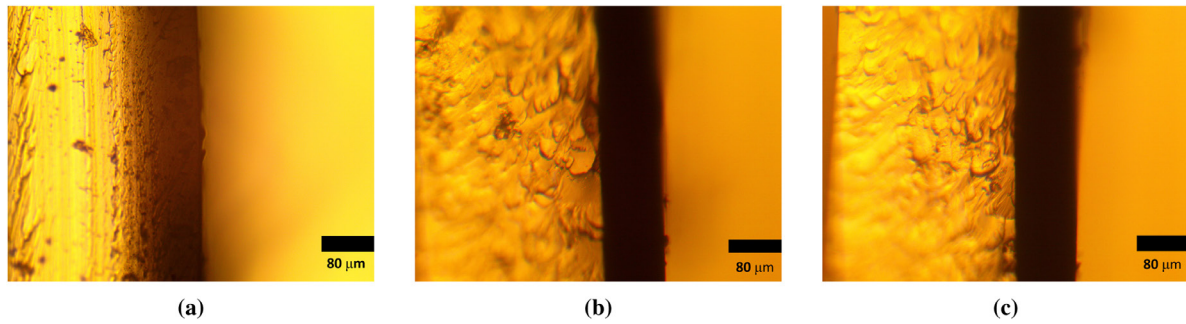


Figure 11. Cross-section images from different curing methods for samples with 1 wt% of CB. (a) Curing method 2, (b) curing method 4 and (c) curing method 6.

t_d based on change of the resistance for each of the samples, we can estimate t_d for all samples. It should be mentioned that the effective diffusion depth is different with the actual diffusion depth. The effective diffusion depth is defined for being able to compare the results. To do so, we compared the resistance of the samples with different thickness before and after curing the PDMS. We performed the calculation with methods 1 and 2.

As we know:

$$R = \frac{\rho l}{wt}. \quad (1)$$

So, making a relation with the initial resistance, R_0 , and the final resistance R_f , assuming an initial thickness t_0 , a constant length, l , and width, w , and a final thickness t_f , it can be calculated the t_d as $t_d = t_0 - t_f$, or:

$$t_d = t_0 - R_0 \times \frac{t_0}{R_f}. \quad (2)$$

As can be seen from tables 3 and 4, for each method, the t_d is almost equal for all samples. That is, for method 1, samples with different thickness (0.35, 0.4 and 0.6) have all an equal effective diffusion depth of 0.23 ± 0.01 mm. and for the method 2, this is 0.29 ± 0.02 mm. This means the actual resistance of each sample produced by each method, can be calculated by

$$R = \frac{\rho l}{w \times (t - t_d)} \quad (3)$$

while the t_d of each fabrication method can be estimated by one experiment. Also, as it was expected the t_d for the method 1, in which the the samples are cured in the oven, is lower than the t_d of the samples with method 2.

To have a better understanding of this diffusion hypothesis, we looked at the cross section of samples prepared by method 2, 4, and 6 with optical microscopy. The images are prepared based on the transmittance of light through a sample. Samples were prepared with lower concentration of carbon black—as low as 1 wt%—that allows light to pass through the sample in less populated areas. From each curing method, 1 mm wide samples were carefully cut and laterally placed on the microscope bench, to observe the cross section under the microscope. Furthermore, in order to enhance the migration of material all samples were cured at room temperature, allowing

Table 5. R_2 is the resistance after three months and R_1 the original resistance, after 144 h. Average values of four samples.

Curing method	Avg R_2/R_1 (16 wt%)	Avg R_2/R_1 (25 wt%)
1	1.29	1.03
2	2.41	1.93
3	1.76	1.06
4	1.09	1.08

higher diffusion time, which corresponds to curing methods 2, 4 and 6. We expect to see a transparent area, corresponding to PDMS, and a dark area that corresponds to cPDMS.

Figure 11 shows the cross section of three samples prepared by curing methods 2, 4 and 6. As can be seen in figures 11(b) and (c), for curing methods 4 and 6, the transition between cPDMS and PDMS is sharp and there is a clear border separating PDMS and cPDMS. However, for curing method 2, (figure 11(a)), the border is not abrupt. There is a visible gradient on the cPDMS, starting more transparent on the border, to more dark in the edge. Comparing the images with the results obtained by the study of the loss of conductivity, we can observe that the images are consistent with the conclusions drawn. The worst curing method is when the PDMS is cast over a cured cPDMS layer for both cases as a result of the migration of PDMS monomers into the cured cPDMS.

5.2. Resistance measurement after three months

In order to further analyze the resistance stability of the samples in a long time, their resistance was measured again after three months. Here, we analyze the ratio between the resistance of the samples measured after three months, R_2 , over the resistance measured after 144 h, R_1 . In this way, we can investigate if the change of the resistance was stabilized or not. Table 5 shows the results for curing methods 1 to 4 for a CB percentage of 16% and 25%, both average value of four samples for each method.

To study the long term durability of these samples, samples with a thickness larger than the effective diffusion depth were chosen. Therefore, all the samples thinner than 0.25 mm were ignored, which means that methods 5 and 6 were not analyzed here.

As can be seen in table 5, for samples with 16%, despite the fact that they are relatively stable after 24 h for some of the

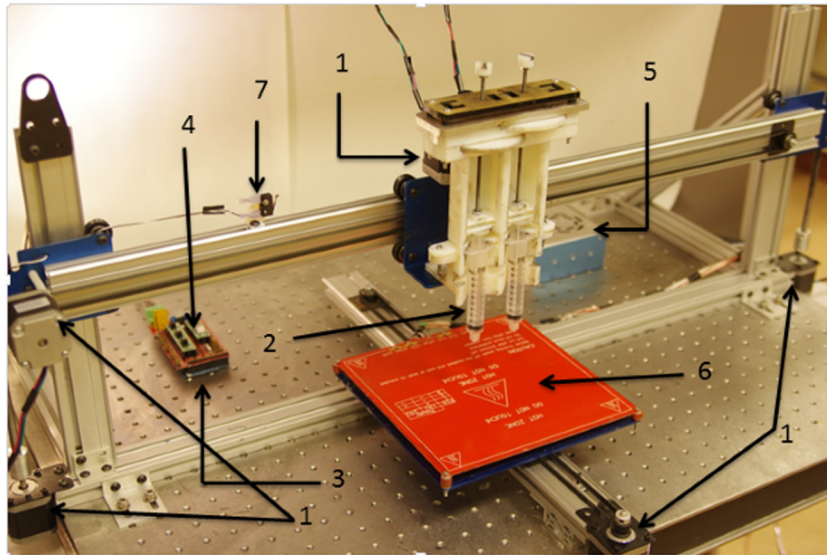


Figure 12. SML 3D printer with extrusion-based syringe deposition. Legend: (1) DC stepper motors; (2) syringes; (3) Arduino Mega; (4) motherboard (Ramps 1.4); (5) mechanical end-stop microswitches; (6) heated printing bed; (7) power supply.

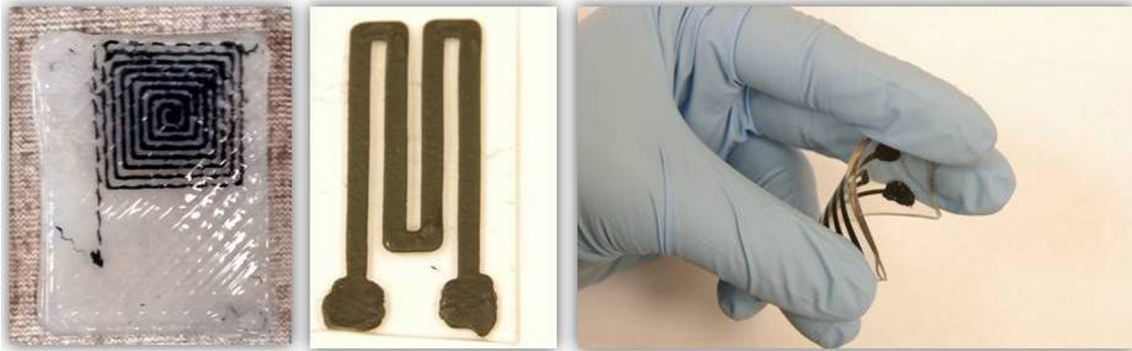


Figure 13. Sample prints of soft electronics with carbon based cPDMS achieved by the SML 3D Printer.

methods, it can be verified that none of the methods had stabilized resistance, and all samples continued to increase their resistance even after three months, while for samples with 25%, some of the methods showed stability. The first take-home is that the CB concentration should be considerably higher than the percolation threshold to have long term stability.

Looking at table 5, one can see that samples with 25% (the curing methods 1, 3 and 4) present very stable behavior (in average 3%, 6% and 8% of increase on resistance after three months). However, as expected, for method 2, where PDMS was cured at room temperature over the cPDMS, the average resistance almost doubled in three months. In addition, also for samples with 16%, the worst case is still method 2, and thus the take home is that for long stability, either for 16% or 25% CB, pouring PDMS pre-polymer over cPDMS should be avoided.

5.3. Improved durability for cPDMS

It is shown that the durability of the conductivity of the cPDMS depends on several factors. First of all, when possible, a higher concentration of CB on PDMS (e.g. over 20%

weight) is recommended. The higher concentration proved to be less prone to loss of the conductivity, since even a small diffusion cannot devastate the percolating CB network. Second, since the diffusion happens up to a limited depth, when possible thicker cPDMS is preferred. In any case, the first two recommendations have disadvantages, and both of them are undesired for many applications. Third, if possible, the cPDMS and PDMS should cure together (not one before the other). Fourth, if the previous method is not possible, PDMS should be cured before cPDMS and not vice versa. Fifth, in all cases curing at the oven gives better results than curing at room temperature. Finally, an Urethane insulator may replace the PDMS. Even though the bonding between PDMS and Urethane is not very good, it is possible to sandwich a cPDMS pattern between two films of Urethane.

5.4. Implication for fabrication techniques and 3D printing

Based on this analysis, we can draw some conclusions that will be useful for the operation of the SML soft electronics additive manufacturing machine. An example of a 3D printer for producing cPDMS-based electronics and sample prints of

soft electronics with this machine are presented in figures 12 and 13. The printer relies on a motorized syringe extrusion-based technique: two different syringes, one carrying PDMS and another cPDMS, act in conjunction with a heated printing bed in order to produce the desired patterns. The hardware interfaces with the computer host through an Arduino Mega and a specialized motherboard (Ramps 1.4). First of all, recall that because the operating principle is based in extrusion syringes, the materials on their inside are necessarily in an uncured stage. This causes a general technical difficulty in additive manufacturing due to the polymers having a low viscosity which causes them to spread when deposited on the printing table. Consequently, we are interested in curing each layer before adding a new one. However, this is not always a good idea due to the negative effects on the conductance.

When depositing the first layer of PDMS, the machine should wait until this layer cures before pouring the uncured cPDMS on top, effectively mimicking methods 5 and 6 depending on the curing temperature used. However, quickly after adding the cPDMS pattern and without waiting for the cPDMS to cure, an additional top layer of PDMS must be deposited over the cPDMS for them to cure together (in a similar way to methods 3 and 4). This is possible because cPDMS has a higher viscosity and does not lose its integrity after adding the top PDMS layer. In short, methods 5/6 would develop between the bottom layer and the cPDMS, and methods 3/4 between the cPDMS and the top PDMS layer. This is the procedure that guarantees long lasting cPDMS tracks, considering the technical limitations imposed by the viscosity of the uncured polymers.

Based on this fact, we enhanced the early version of the printer with a heating bed (figure 13). In this way, the layers are cured based on the priority order explained above.

6. Conclusion

In this article, we evaluated the effect of composition, layer thickness, curing order and curing temperature, and some insulating materials on the change of the conductivity on soft and stretchable electronics that are composed of PDMS and cPDMS layers. We found out that the change on the conductivity is happening due to the diffusion process between the PDMS and cPDMS layers. We also show that by calculating the effective diffusion depth for each fabrication method, the eventual resistance of the tracks can be calculated. From the interpretation of the results we suggested that such diffusion can make the cPDMS less populated with conductive particles, thus resulting in the loss of conductance. However, by careful selection of the diffusion parameters one can limit the effective diffusion depth, and thus limit the changes on the conductance. Conductive cPDMS tracks with lower changes on their resistance are obtained when curing cPDMS and PDMS layers together at high temperatures, or if the PDMS is cured before integration of the cPDMS. In all cases, deposition of an uncured PDMS over cured cPDMS should be avoided as much as possible. These findings can help in the design of the fabrication process both by manual or additive manufacturing

methods, so that the conductivity of the cPDMS layer can be maintained fix for long time. For the SML 3D printer module, we updated the printer with a heated bed, to allow fabrication of long lasting conductive traces. Nevertheless, a heat bed works for the first few layers, and is very slow. An ideal process for this machine would be localized and rapid infrared heating of the surface from the top layer.

Acknowledgment

This work was supported by the Portuguese Foundation of Science and Technology and the CMU-Portugal program, under the contract numbers CMUP-EPB/TIC/0036/2013 and CMUP-ERI/TIC/0021/2014.

References

- [1] Hammock M L, Chortos A, Tee B C-K, Tok J B-H and Bao Z 2013 25th anniversary article: the evolution of electronic skin (E-skin): a brief history, design considerations, and recent progress *Adv. Mater.* **25** 5997–6038
- [2] Lipomi D J, Vosgueritchian M, Tee B C-K, Hellstrom S L, Lee J A, Fox C H and Bao Z 2011 Skin-like pressure and strain sensors based on transparent elastic films of carbon nanotubes *Nat. Nanotechnol.* **6** 788–92
- [3] Dickey M D 2014 Emerging applications of liquid metals featuring surface oxides *ACS Appl. Mater. Interfaces* **6** 18369–79
- [4] Rogers J A, Someya T and Huang Y 2010 Materials and mechanics for stretchable electronics *Science* **327** 1603–7
- [5] Lee M-S et al 2013 High-performance, transparent, and stretchable electrodes using graphene–metal nanowire hybrid structures *Nano Lett.* **13** 2814–21
- [6] An B W, Hyun B G, Kim S-Y, Kim M, Lee M-S, Lee K, Koo J B, Chu H Y, Bae B-S and Park J-U 2014 Stretchable and transparent electrodes using hybrid structures of graphene–metal nanotrough networks with high performances and ultimate uniformity *Nano Lett.* **14** 6322–8
- [7] Matsuhisa N, Kaltenbrunner M, Yokota T, Jinno H, Kuribara K, Sekitani T and Someya T 2015 Printable elastic conductors with a high conductivity for electronic textile applications *Nat. Commun.* **6** 7461
- [8] Lorussi F, Scilingo E P, Tesconi M, Tognetti A and De Rossi D 2005 Strain sensing fabric for hand posture and gesture monitoring *IEEE Trans. Inf. Technol. Biomed.* **9** 372–81
- [9] Weigel M, Lu T, Bailly G, Oulasvirta A, Majidi C and Steimle J 2015 Iskin: flexible, stretchable and visually customizable on-body touch sensors for mobile computing *ACM Conf. Hum. Factors Comput. Syst.* pp 2991–3000
- [10] Lu T, Finkenauer L, Wissman J and Majidi C 2014 Rapid prototyping for soft-matter electronics *Adv. Funct. Mater.* **24** 3351–6
- [11] Spahr M, Gilardi R and Bonacchi D 2014 Carbon black for electrically conductive polymer applications *Encyclopedia of Polymers and Composites* (Berlin: Springer) pp 1–20
- [12] Oskuoyi A, Sundararaj U and Mertiny P 2014 Tunneling conductivity and piezoresistivity of composites containing randomly dispersed conductive nano-platelets *Materials* **7** 2501–21
- [13] Stassi S, Cauda V, Canavese G and Pirri C 2014 Flexible tactile sensing based on piezoresistive composites: a review *Sensors* **14** 5296–332

- [14] Huang J-C 2002 Carbon black filled conducting polymers and polymer blends *Adv. Polym. Technol.* **21** 299–313
- [15] Noordemeer J and Dierkes W 2015 Carbon black reinforced elastomers *Encyclopedia of Polymeric Nanomaterials* (Berlin: Springer) pp 1–14
- [16] Tavakoli M, Rocha R, Lourenco J, Lu T and Majidi C 2017 Soft bionics hands with a sense of touch through an electronic skin *Springer* **17** 5–10
- [17] Tavakoli M and de Almeida T 2014 Adaptive under-actuated anthropomorphic hand: ISR-softhand 2014 *IEEE/RSJ Int. Conf. on Intelligent Robots and Systems* pp 1629–34
- [18] Tavakoli M, Batista R and Sgrigna L 2015 The UC softhand: light weight adaptive bionic hand with a compact twisted string actuation system *Actuators* **5** 1 (Multidisciplinary Digital Publishing Institute)
- [19] Cianchetti M and Mensiassi A 2017 Soft robots in surgery *Soft Robotics: Trends, Applications and Challenges* vol 17 (Springer International Publishing) pp 75–85
- [20] Beccai L, Lucarotti C, Totaro M and Taghavi M 2017 Soft robotics mechanosensing *Soft Robotics: Trends, Applications and Challenges* vol 17 (Springer International Publishing) pp 11–21